Proceedings of the 8th National Congress on Theoretical and Applied Mechanics, May 28-29, Brussels, Belgium.

Chip Formation in Micro-milling

F. Ducobu, E. Filippi, E. Rivière-Lorphèvre
Service de Génie Mécanique, Faculté Polytechnique de Mons
Rue du Joncquois 53, B-7000 Mons - Belgium
Email: Francois.Ducobu@umons.ac.be, Enrico.Filippi@umons.ac.be, Edouard.Riviere@umons.ac.be

Abstract— **In the current context of miniaturisation, micro-machining processes are in full expansion. One of them is micro-milling, able to produce parts with features ranging from several** mm **to several** µm**.**
Despite the down-sizing of the macro-milling process, micro-cutting is not a simple scaling-down of macro-cutting. The new way of forming chips involves the so-called 'minimum chip thickness' phenomenon, below which no chip is formed. Estimating the minimum chip thickness value is one of the main challenges in micro-milling. A review of the current state-of-the-art in chip formation and minimum chip thickness in micro-milling is reported in this paper from an experimental and numerical point of view.
In order to model the chip formation process, 2D numerical simulations are performed using the finite element method and a commercial software programme, ABAQUS/Explicit v6.7. The Lagrangian formulation has been adopted and a chip separation criterion is used to make chip formation possible. Results of the finite element simulations are presented and compared to results found in the literature.

Keywords—**Micro-milling, chip formation, minimum chip thickness, orthogonal cutting**

I. Introduction

FOR a few years, the tendency towards miniaturisation has been gaining in importance and affects many fields, involving an increasing demand for micro-components. A growing development of micro-manufacturing techniques is consequently observed. Micro-milling is one of them. It consists in a micro-machining process using a cutting tool (called a 'micro-mill', typical diameter between 100 µm and 500 µm) rotating at a high speed to remove material from the workpiece and making it possible to produce parts and features between some mm and some µm [1], [2] and [3]. Up to now micro-milling seemed to be the most flexible and fastest way to produce complex tridimensional micro-forms, including sharp edges, with a good surface quality in many materials: metal alloys, composites, polymers and ceramics [4]. Its applications are quite varied, to cite a few: micro-injection moulds, watch components, optical devices, components for the aerospace, biomedical and electronic industries.

In order to present the main differences in chip formation due to the scaling-down from macro- to micro-milling, a short review of the current state of the art in chip formation and minimum chip thickness in micro-milling is carried out. Then the finite element model developed is presented, before commenting and comparing our results to those found in the literature.

II. Chip formation specificities in micro-milling

A. Minimum Chip Thickness

IN micro-milling the depth of cut and the feed per tooth are very small (of the same order of magnitude as the tool edge radius) and no chip is formed below a value called 'minimum chip thickness'. Chae et al. [1] define it as the critical depth of cut (between 5% and 38% of the tool edge radius, depending on the machined material [5]) below which no chip can be formed. Three different cases happen in micro-chip formation, as shown on Figure 1 (R: edge radius, h: depth of cut, h_m: minimum chip thickness).

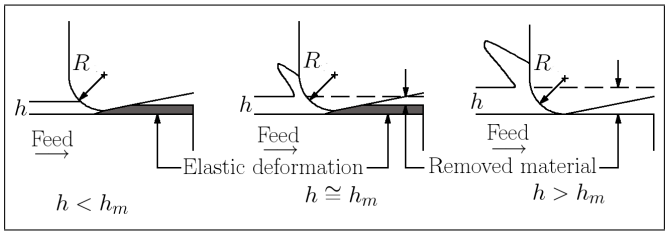

Fig. 1. Schematic representation of the minimum chip thickness in orthogonal cutting, inspired from [1]

Increase of cutting forces, burr formation and surface roughness are the consequences of the rise of slipping forces and the ploughing of the machined surface (highlighted by Bissacco et al. [6]) due to the minimum chip thickness phenomenon. Hence minimum chip thickness values must be determined and taken into account to choose adequate cutting parameters. Machined material and tool geometry greatly affect the minimum chip thickness value, complicating its estimation [7].

B. Negative Rake Angle

The macro-cutting assumption stating that the tool is sharp, completely cuts the surface and generates chips is not valid in micro-cutting. This is due to the highly negative rake angle caused by the small depth of cut being of the same order of magnitude as the tool edge radius (Fig-

ure 2). A highly negative rake angle leads to ploughing of the machined surface and elastic spring back of the workpiece. The spring back fraction occurring under the flank face leads to friction, raising the specific cutting energy.

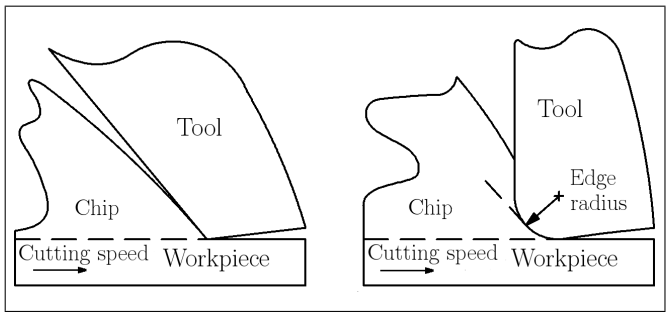

Fig. 2. Schematic representation of the negative rake angle in orthogonal cutting, inspired from [2]

C. Size Effect

At a small depth of cut, Filiz et al. [8] observed the so-called 'size effect': a decrease in the depth of cut leads to a non-linear increase in the specific cutting energy. Minimum chip thickness and specific cutting energy are thus closely related. The specific cutting energy could be an indicator making it possible to detect changes (from slipping to shearing) in the cutting mechanism and to monitor the process.

D. Influence of the Machined Material

In micro-milling, as the dimensions of the depth of cut, the tool or feature to produce are often smaller than the grain size of the machined material, its nature and micro-granular structure have to be taken into account [1] and [2]. Therefore it can no longer be considered as homogeneous and isotropic, contrary to the assumption made in macro-machining. The microstructure of the machined material takes on great importance in micro-milling.

Chae et al. [1] and Dornfeld et al. [2] report variations in cutting forces and vibrations during micro-machining due to the lack of homogeneity of the workpiece granular structure. This leads to variations in cutting condition (hardness in particular). Modifying the cutting conditions or the machine design is not a solution to eliminate them, as they are due to the nature of the machined material. Finally, averaged cutting coefficients from macro-cutting cannot be used any more.

E. Numerical Works

Up to now, very few numerical works about minimum chip thickness can be found in the literature.

A 2D ALE orthogonal cutting finite element model was developed by Woon et al. [9] in order to study the influence of the tool edge radius on chip formation. This model considers the workpiece material (AISI 4340 steel) as homogeneous and the tool is modelled as a perfectly rigid solid with and without edge radius. The results of their research show that the chip is formed by extrusion along the tool edge radius when the depth of cut is lower than a breaking value and confirm that the tool cannot be considered sharp in micro-milling.

In order to study the influence of the granular structure of the machined material on chip formation, Simoneau et al. [10] developed a 2D Lagrangian orthogonal cutting heterogeneous (AISI 1045 steel) finite element model with a sharp tool. They observed a new chip formation mechanism (Figure 3): the softest material (ferrite) is extruded between the hardest grains (pearlite). They called it a 'quasi-shear extrusion chip'. This shows that it is crucial to model the workpiece material as heterogeneous in micro-cutting.

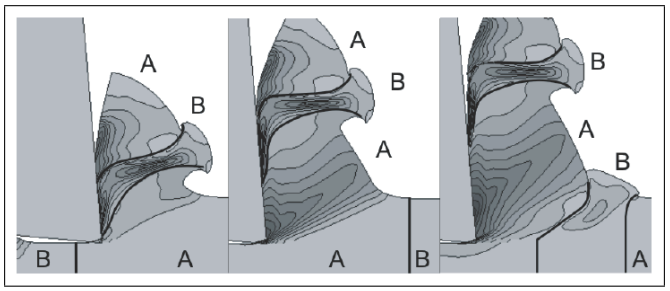

Fig. 3. AISI 1045 steel numerical chip formation (A: pearlite, B: ferrite) [10]

III. Numerical Model

THE chip formation is studied with a 2D plane strain orthogonal cutting model developed with the commercial software programme ABAQUS/Explicit v6.7. It only takes into account the area close to the cutting edge of the tool.

An explicit Lagrangian formulation is adopted as our interest is focused on the transient phase of the chip formation and the cutting refuse. Moreover the model must be able to produce saw-tooth chips, which cannot be achieved with an Arbitrary Lagrangian Eulerian (A.L.E.) formulation, contrary to Lagrangian formulation [11].

For a determined material, the minimum chip thickness depends on the depth of cut (h) and the cutting edge radius of the tool (r). Various h/r ratios have been considered in order to study the influence of the depth of cut on the chip formation process. Ten different cases have been simulated from $h/r = 5$ ($h = 100$ µm) to $h/r = 0.05$ ($h = 1$ µm): $h/r = 5$, 3, 1, 0.5, 0.375, 0.25, 0.2, 0.15, 0.1 and 0.05.

A. Overview

The workpiece is modelled as a rectangular block, while the tool is modelled with a 20 µm cutting edge radius, a 0° rake angle and a 5° clearance angle. The cutting speed is set to 300 m/min. The workpiece and the tool are meshed with three- and four-node linear elements. Figure 4 presents the initial geometry and mesh of the model when $h/r = 5$ (H: horizontal degree of freedom constrained, V: vertical degree of freedom constrained).

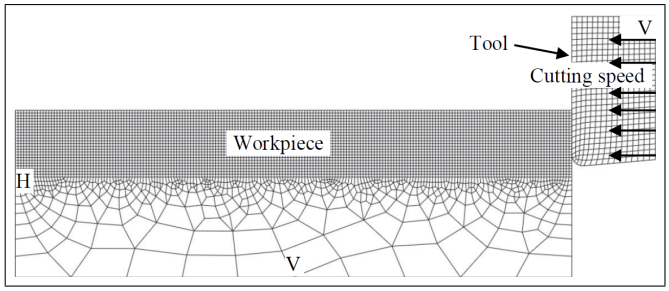

Fig. 4. Boundary conditions and initial mesh when $h/r = 5$

The workpiece material is a titanium alloy, Ti6Al4V, assumed to be homogeneous. Its behaviour is described by the Johnson-Cook plasticity model [12]. The tool material, tungsten carbide, is also homogeneous and its behaviour is described by a linear elastic law.

Friction at the chip - tool interface is implemented using a limiting shear friction model with a limiting shear stress and a friction coefficient [13]. All of the friction energy is converted into heat and 25% of this friction heat flows into the workpiece [14].

The two parts initial temperature is set to 20°C. Only conduction is considered and all the workpiece faces are adiabatic [15]. The efficiency of the deformation to heat transformation is assumed to be 90% [9], [13] and [14].

B. Chip Separation Criterion

Due to the Lagrangian formulation, a chip separation criterion based on an 'eroding element' method is introduced in the model to make chip formation possible. This separation criterion is based on crack propagation depending on the stress and strain state of the machined material. This chip formation approach, by ductile failure phenomenon, is composed of two steps.

In the first step, a damage initiation criterion must be fulfilled. The damage initiation criterion adopted is the Johnson-Cook shear failure model [12].

The second step concerns damage propagation, based on the fracture energy approach. This criterion uses the fracture energy, G_f, which is the energy required to open a unitary area crack. After damage initiation, the material behaviour is represented by a stress-displacement relation rather than a stress-strain relation [15]. As soon as the specified value of G_f is reached in a finite element, it is deleted and all of its stress components are put to zero. The suppression of a finite element introduces a crack in the workpiece, making it possible for the chip to come off.

IV. Results

A. Chip Formation and Morphology

Figures 5 to 10 show chip formation and machined material deformation for various h/r ratios values. A chip is undoubtedly formed when $h/r = 5$ to 0.375, which is not true for $h/r = 0.25$ to 0.05. Therefore it could be interesting to establish a criterion making it possible to give a ruling on the existence of a chip. An interesting point is the presence of a saw-tooth chip when $h/r = 5$ and 3, as observed experimentally in macro-cutting. This kind of chip is not found any more for smaller simulated h/r values. This can be due to the h/r ratio value or even to the short simulation time (some microseconds).

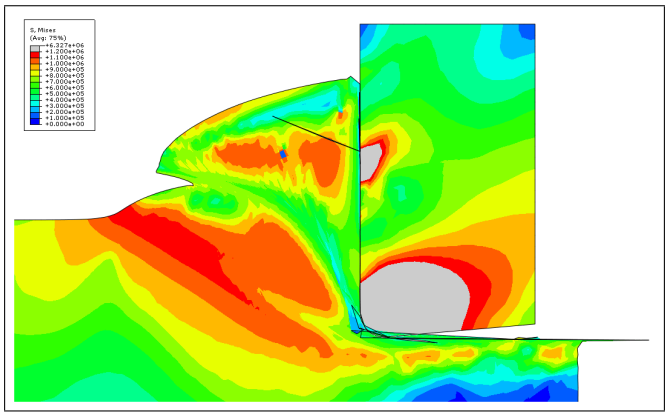

Fig. 5. Von Mises stress contours (10^3 Pa) during chip formation when $h/r = 5$

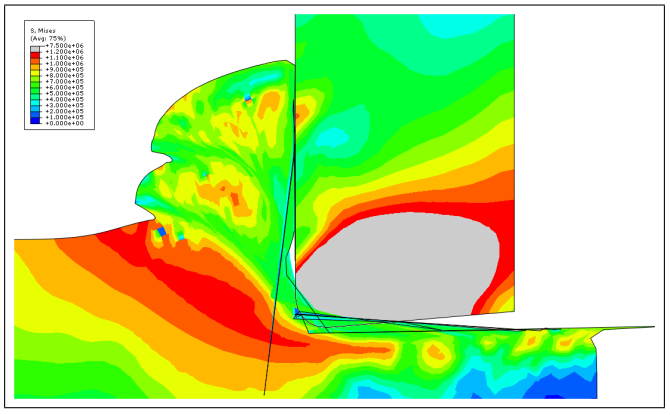

Fig. 6. Von Mises stress contours (10^3 Pa) during chip formation when $h/r = 3$

A primary shear zone is clearly visible on Von Mises stress contours when $h/r = 5$ and 3, as in macro-cutting

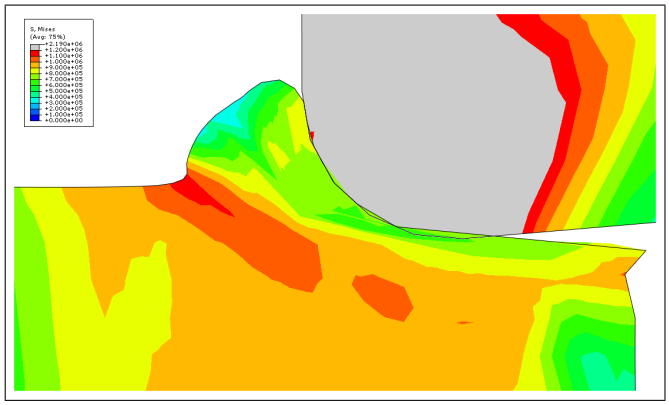

Fig. 7. Von Mises stress contours (10^3 Pa) during chip formation when $h/r = 0.375$

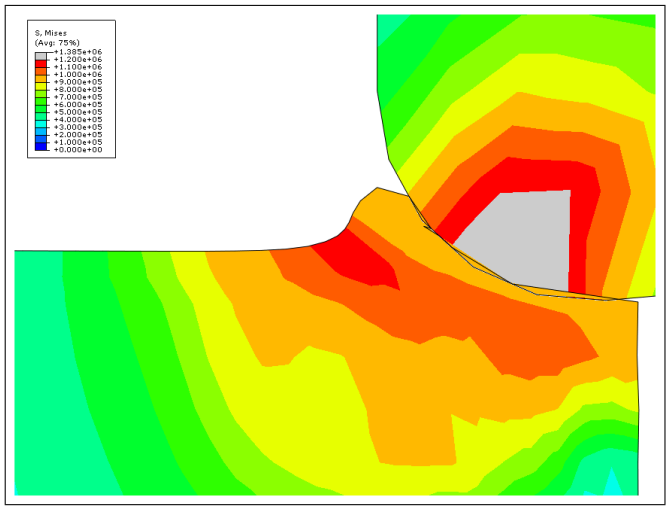

Fig. 8. Von Mises stress contours (10^3 Pa) during chip formation when $h/r = 0.25$

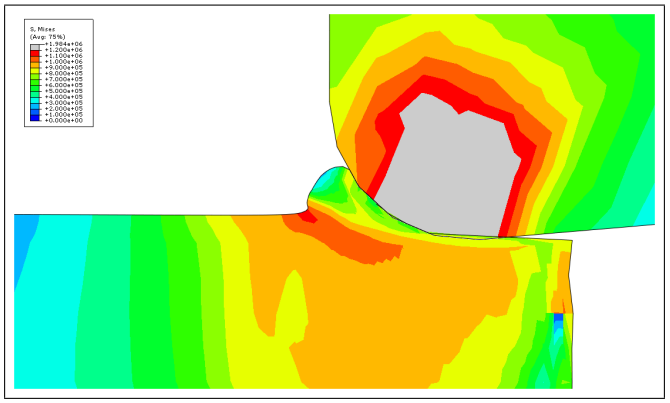

Fig. 9. Von Mises stress contours (10^3 Pa) during chip formation when $h/r = 0.2$

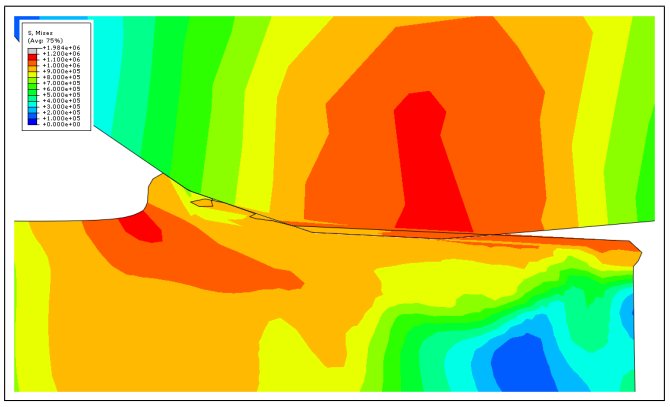

Fig. 10. Von Mises stress contours (10^3 Pa) during chip formation when $h/r = 0.05$

with a sharp tool. The more the h/r ratio decreases, the more the primary shear zone fades and it cannot be distinguished any longer from the $h/r = 0.25$ value. It is interesting to highlight that the $h/r = 0.375$ value could be a key value. Indeed a primary shear zone can still be seen but the stress value seems to be smaller.

These results are globally similar to those presented by Woon et al. [9] in the case of an A.L.E. model. Actually the cutting tool can no longer be considered as sharp and the h/r value has a great influence on the chip formation in micro-cutting. Changes in the chip formation mechanism are observed when the h/r ratio decreases, evolving away from macro-cutting.

B. Cutting Forces

Figure 11 shows the cutting and the feed forces for a 100 µm depth of cut. A cyclic evolution can be observed, as expected due to the saw-toothed chip. Indeed when the formation of a slipping plane occurs (corresponding to a tooth formation), a drop in the forces is observed. It also must be highlighted that the cutting force is greater than the feed force, which is also observed in macro-cutting.

Figure 12 represents the evolutions of the ratio between feed and cutting forces for the ten h/r simulated ratios. The $h/r = \infty$ value stands for the theoretical forces ratio value when the tool is infinitely sharp. The more the h/r ratio decreases, the more the forces ratio increases. When the h/r ratio becomes smaller than the unit, the feed force becomes greater than the cutting force. A change in the cutting mechanism is thus observed: an inversion between cutting and feed forces has occurred. These observations are similar to those made experimentally by Liu et al. [3].

Three different situations can be seen on Figure 12. When the h/r ratio value evolves between 5 and 1 the feed to cutting forces ratio is less than 1, as in macro-cutting. On the contrary from h/r values for 0.05 to 0.2, the forces ratio tends to 2. The three remaining h/r ratio are found between the forces ratio values 1 and 2. With a feed to cutting forces ratio criterion value of 2, the minimum chip thickness value would be between 4 µm and 7.5 µm.

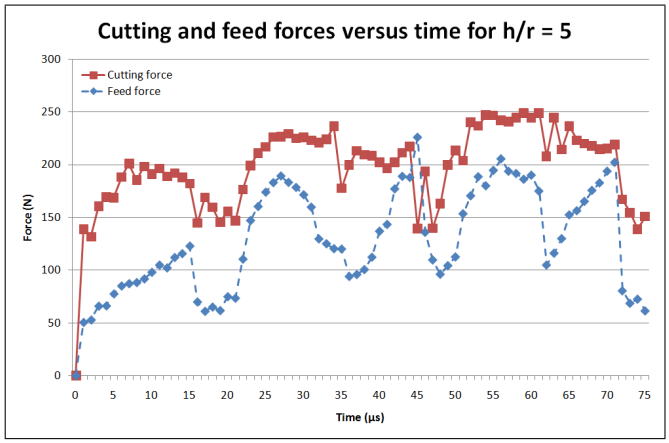

Fig. 11. Force evolutions during cutting when $h/r = 5$

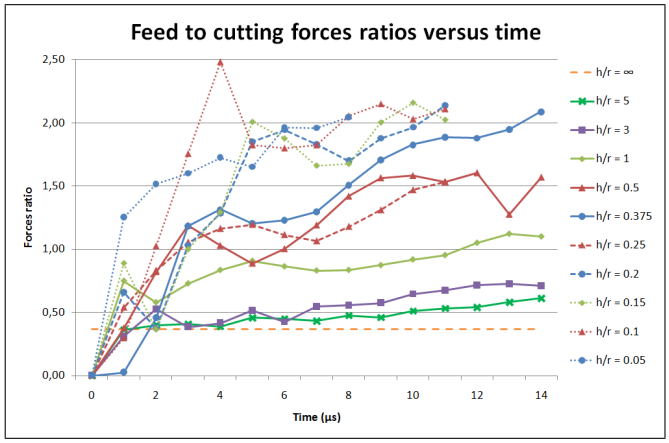

Fig. 12. Force ratio evolutions during cutting for various h/r ratios

C. Specific Cutting Energy

The evolutions of the ratio between the specific cutting energy and the theoretical specific cutting energy when the tool is infinitely sharp can be seen on Figure 13 for the ten simulated h/r ratios. For $h/r = 5$ and 3, the average value of the specific cutting energy value is close to the theoretical one. A non-linear rise in the specific cutting energy is noticed when the depth of cut decreases, in accordance with the previously presented size effect phenomenon.

Again, different cases are observed depending on the h/r value. The two h/r ratio values at both ends of the simulated range lead to specific cutting energy ratios that are clearly different. With a specific cutting energy ratio criterion value of 2, the minimum chip thickness would lie between 2 µm and 7.5 µm.

D. Vertical Displacement

The evolutions of the vertical displacement of a particular node is studied in this section for each simulated h/r ratio. For $h/r = 5$ and 3 (first situation on Figure 14), the

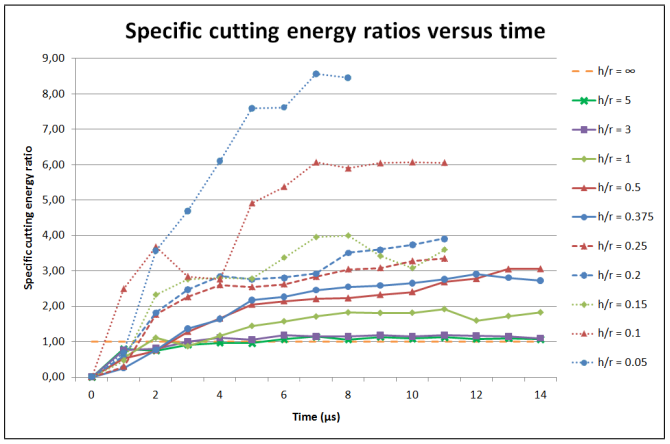

Fig. 13. Specific cutting energy ratio evolutions during cutting for various h/r ratios

node considered is the one situated at the same level as the upper node of the cutting edge radius of the tool. For h/r equal to or smaller than the unit (second situation in Figure 14), the node considered is the one at the upper right corner of the workpiece.

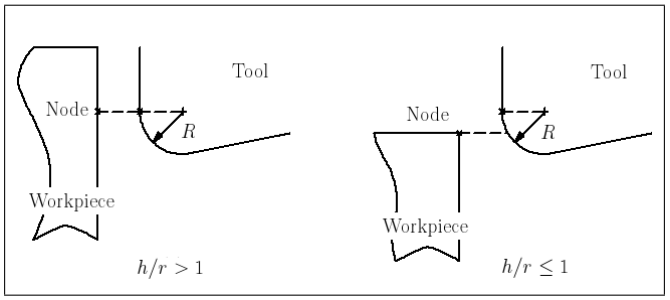

Fig. 14. Schematic localisation of the considered node

The vertical displacement of this particular node is interesting because a negative vertical displacement value means that no chip is formed and that the workpiece material is deformed and flows under the cutting edge of the tool (as in the first case of Figure 1). On the other hand a positive vertical displacement value means that a chip is formed.

Figure 15 shows that when h/r is smaller than 0.15 the vertical displacement is negative. For h/r values greater than 0.375, the vertical displacement is positive (the vertical displacement when $h/r = 1$ seems strangely large). The vertical displacement in the two remaining cases is not strictly positive or negative. The minimum chip thickness value in accordance with the node's vertical displacement would be between 3 µm and 5 µm.

E. Minimum chip thickness prediction

Each method results in a different range of probable minimum chip thickness values (Figure 16). The resultant

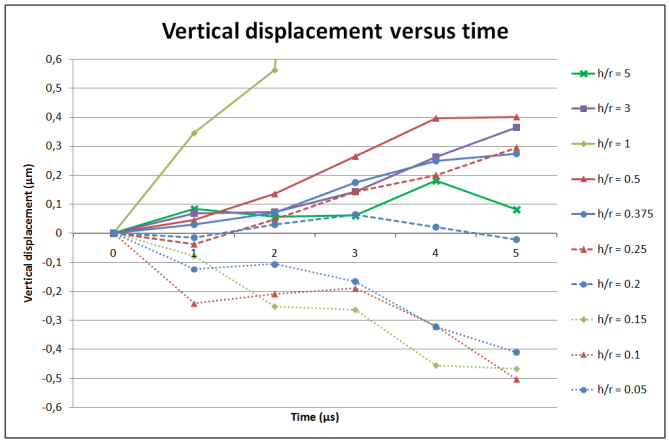

Fig. 15. Vertical displacement evolutions during cutting for various h/r ratios

of these three ranges is 4-5 µm (or 20-25% of the cutting edge radius of the tool). This can be considered as a first approximation of the minimum chip thickness value for Ti6Al4V with the geometry and the cutting condition of the model.

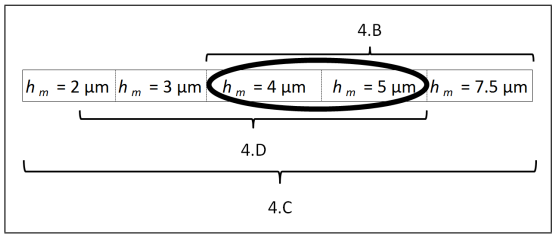

Fig. 16. Minimum chip thickness value ranges and resultant

Lastly, highly deformed finite elements can be observed during simulations. Those are not removed, contrary to what was expected. Some of them can be seen in the previous figures: they are the black lines interfering with the workpiece and the chip near the edge radius of the tool. This problem has to be solved.

V. Conclusions

CHANGES in the cutting phenomenon are induced by the transition from macro- to micro-milling. One of these changes is the chip formation involving the minimum chip thickness phenomenon, which has been reported in this paper.

The influence of the depth of cut on chip formation has been studied with the developed numerical model. A decrease in the depth of cut leads to changes in the cutting process mechanism and the cutting tool can no longer be considered sharp, contrary to the assumption with macro-cutting.

An evolution in the cutting to feed forces ratio has been highlighted when the depth of cut decreases. Beyond a critical value of the depth of cut (10 µm in this paper) the feed force becomes greater than the cutting force. This inversion could be used to determine the minimum chip thickness value.

It has also been observed that the depth of cut value greatly affects the specific cutting energy. Indeed it rises when the depth of cut decreases, which is known as the size effect. The minimum chip thickness value could be determined thanks to the evolution of the specific cutting energy.

Finally the vertical displacement of a particular node has been studied in order to determine if the machined material flows under the cutting edge of the tool instead of forming a chip. A small depth of cut (less than 4 µm in this paper) leads to a negative vertical displacement of the node. The transition from a positive to a negative vertical displacement could help in determining the minimum chip thickness value.

Each of the three methods ends in a different range of probable minimum chip thickness values, the intersection of them being 4-5 µm. The value of the minimum chip thickness for Ti6Al4V with the geometry and the cutting condition of the model is estimated at 4-5 µm, i.e. 20-25% of the cutting edge radius of the tool.

References

[1] Chae J., Park S., and Freiheit T., *Investigation of micro-cutting operations*, IJMTM, 45, 313–332, 2006.

[2] Dornfeld D., Min S., and Takeuchi Y., *Recent advances in mechanical micromachining*, Annals of the CIRP, 55, 745–768, 2006.

[3] Liu X., DeVor R., Kapoor S., and Ehman K., *The mechanics of machining at the micro scale: assessment of the current state of the science*, JMSE, 126, 666–678, 2004.

[4] Weule H., Hüntrup V., and Trischler H., *Micro-cutting of steel to meet new requirements in miniaturization*, Annals of the CIRP, 50:61–64, 2001.

[5] Ohbuchi Y. and Obikawa T., *Finite element modeling of chip formation in the domain of negative rake angle cutting*, ASME, 125, 324–332, 2003.

[6] Bissacco G., Hansen H.N., and De Chiffre L., *Size effect on surface generation in micromilling of hardened tool steel*, Annals of the CIRP, 55:593–596, 2006.

[7] Liu X., DeVor R., and Kapoor S., *An analytical model for the prediction of minimum chip thickness in micromachining*, ASME, 128, 474–481, 2006.

[8] Filiz S., Conley C., Wasserman M., and Ozdoganlar O., *An experimental investigation of micro-machinability of copper 101 using tungsten carbide micro-endmills*, IJMTM, 47, 1088–1100, 2007.

[9] Woon K., Rahman M., Fang F., Neo K., and Liu K., *Investigations of tool edge radius effect in micromachining: a FEM simulation approach*, JMPT, 167, 316–337, 2007.

[10] Simoneau A., Ng E., and Elbestawi M.A., *The effect of microstructure on chip formation and surface defects in micro-scale, mesoscale, and macroscale cutting of steel*, Annals of the CIRP, 55:97–102, 2006.

[11] Ducobu F., *Thèse de Doctorat – Etude du phénomène de coupe en micro-fraisage par enlèvement de copeaux: Rapport de réunion*

du 04/02/2009, Technical report, Faculté Polytechnique de Mons, 2009.

[12] Johnson G. and Cook W., *Fracture characteristics of three metals subjected to various strains, strain rates, temperature and pressures*, EFM, 21, 31–48, 1985.

[13] Özel T. and Zeren E., *Numerical modelling of meso-scale finish machining with finite edge radius tools*, IJMMM, 2, 451–768, 2007.

[14] Nasr M., Ng E.-G., and Elbestawi M., *Effects of workpiece thermal properties on machining-induced residual stresses - thermal softening and conductivity*, Proc. IMechE, Part B: JEM, 221, 1387–1400, 2007.

[15] Mabrouki T., Girardin F., Asad M., and Rigal J.-F., *Numerical and experimental study of dry cutting for an aeronautic aluminium alloy (A2024-T351)*, IJMTM, 48, 1187–1197, 2008.